Acta Geophysica (2021) 69:17–27
https://doi.org/10.1007/s11600-020-00519-9

RESEARCH ARTICLE - SOLID EARTH SCIENCES

Discrimination of earthquakes and quarries in the Edirne district (Turkey) and its vicinity by using a linear discriminate function method and artificial neural networks

Aylin Tan[1] · **Gündüz Horasan**[2] · **Doğan Kalafat**[3] · **Ali Gülbağ**[4]

Received: 31 January 2020 / Accepted: 20 November 2020 / Published online: 3 January 2021

Abstract

In this study, seismic events in the Edirne district (Turkey) and its vicinity have been investigated in order to discriminate earthquakes from quarry blasts. A total of 150 seismic events with Md ≤ 3.5 duration magnitude from a seismic activity catalog between 2009 and 2014 recorded by the Enez (ENEZ), Erikli (ERIK) and Gelibolu (GELI) broadband stations operated by Boğaziçi University, Kandilli Observatory and Earthquake Research Institute Regional Earthquake-Tsunami Monitoring Center were used in this study. The maximum S-wave and maximum P-wave amplitude ratio of vertical component velocity seismograms, power ratio (Complexity) and total signal duration of the waveform were calculated. Earthquakes and quarry blasts were discriminated using the linear discriminate function (LDF) and back propagation feed forward neural networks, an artificial neural network (ANN) learning algorithm, taking the determination coefficient and variance account values between these parameters into consideration. Eighty-one (54%) of the total 150 seismic events studied were determined to be earthquakes, and sixty-nine (46%) of them were determined to be quarry blasts. The LDF and ANNs methods were applied to the data in Edirne and its vicinity using a pair of parameters and were compared to each other for the first time. The accuracy of the methods are 95% and 99% for LDF and ANNs, respectively.

Keywords Earthquake · Quarry blast · Linear discriminate function (LDF) · Artificial neural networks (ANNs)

Introduction

While seismic recorders are recording seismic events in a region, they record not only natural seismic activities but also man-made events such as quarry blasts. These events exist in seismicity catalogs together. This situation may cause some errors for scientific studies in these areas, such as in the determination of the *b*-value in seismic hazard studies. In order to determine the real seismic activity in a study area, seismic catalogs should be cleaned of quarry blasts. The use of location, distance and origin time are simply not enough to achieve this. Therefore, waveforms should be carefully examined (Horasan et al. 2006).

Many different methods exist in the literature on the subject of the discrimination of natural and man-made seismic activity. These include the Pn/Sn and Pn/Lg ratio methods (Baumgardt and Young 1990), the Lg/Pg and Lg/Rg ratio methods (Wüster 1993), the artificial neural networks (ANNs) method (Dowla et al. 1990), the linear discriminant function (LDF) method (Horasan et al. 2006, 2009; Deniz 2010; Öğütçü et al. 2010; Kartal 2010; Kekovalı et al. 2010, 2012; Badawy et al. 2019; Ceydilek and Horasan 2019) and short-time Fourier transform (STFT) methods (Yılmaz et al. 2013), quadratic discriminate function (QDF), diquadratic discriminate function (DQDF) and Mahalabonis discriminate function (MDF) methods (Küyük et al. 2011), QDF

Communicated by Ramon Zuñiga, Ph.D. (CO-EDITOR-IN-CHIEF)/Rodolfo Console (ASSOCIATE EDITOR).

✉ Aylin Tan
aylin.tan@ogr.sakarya.edu.tr

1 Natural Sciences Institute, Geophysical Engineering Department, Sakarya University, 54100 Sakarya, Turkey

2 Geophysical Engineering Department, Engineering Faculty, Sakarya University, 54100 Sakarya, Turkey

3 Kandilli Observatory and Earthquake Research Institute Regional Earthquake-Tsunami Monitoring Center, Boğaziçi University, 34000 Kandilli, Istanbul, Turkey

4 Computer Engineering Department, Computer and Information Sciences Faculty, Sakarya University, 54100 Sakarya, Turkey

methods (Yavuz et al. 2018), spectral seismograms (Korrat et al. 2008), declustering-dequarry discriminate methods (Kalafat 2010), the Fisher–Shannon discrimination method (Telesca et al. 2011), the corner frequency discriminant (CFD) method and P- and S- wave corner frequencies (Ataeva et al. 2017), and histograms of time versus seismic events (Naserieh et al. 2019).

In addition to these methods, natural and artificial seismic events have also been distinguished from each other using several algorithms of artificial neural networks (ANNs). In this study seismic activities occurring during May 2009 and March 2014 in Edirne (Turkey) and its vicinity were examined. The location of the stations and the distribution of seismic events are shown in Fig. 1. Most of the quarry blasts recorded in the study area are related to mineral and construction material extraction. The purpose of this study is the discrimination of quarry blasts from earthquakes by applying the linear discriminate function (LDF) and artificial neural networks (ANNs) methods on digital vertical component velocity seismograms recorded at the ERIK, ENEZ and GELI seismic stations. The obtained values of accuracy percentage were compared to determine the real seismic activity. This will improve the quality of earthquake catalogs, help to better determine their completeness, reduce errors in seismic hazard studies by ensuring that quarry sites are not identified as fault zones and allow the calculation of reliable *b*-values.

Data and methods

In this study, a total of 150 seismic events with Md ≤ 3.5 recorded at three stations, ERIK, ENEZ and GELI, were investigated between May 2009 and March 2014 in the region bounded by 40–41° N and 25.30–26.80° E (Fig. 1). Data were taken from Boğaziçi University,

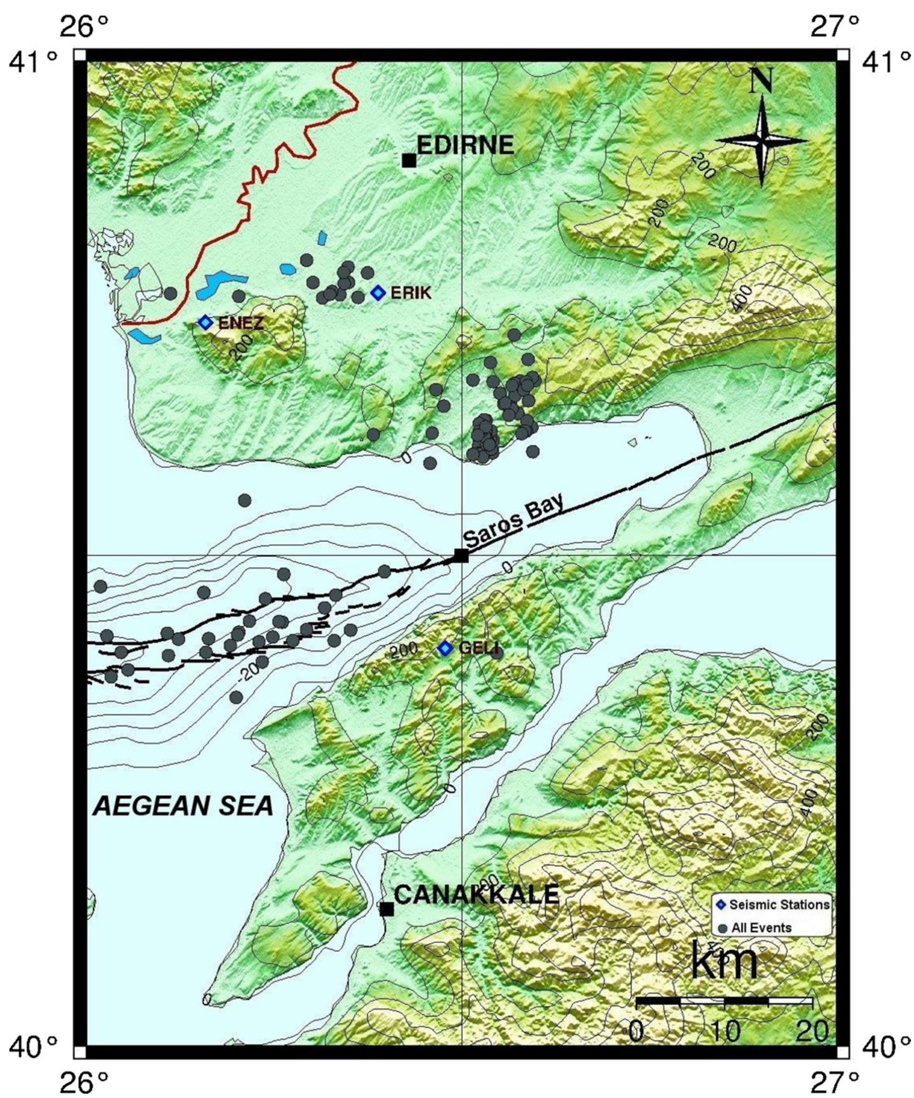

Fig. 1 Location of the stations ERIK, ENEZ and GELI and seismic events with magnitudes of Md ≤ 3.5 in the study area between May 2009 and March 2014 (RETMC). Faults were taken from Şaroğlu et al. (1992), Emre et al. (2013) and Yaltirak et al. (2012). NAFZ: North Anatolian Fault Zone

Kandilli Observatory and Earthquake Research Institute, and the Regional Earthquake–Tsunami Monitoring Center (RETMC).

The vertical component velocity seismogram data recorded at station ENEZ have the lowest number of data points.

The seismic activity distribution versus day and time (in GMT) are shown in Fig. 2. The histogram at the right side of Fig. 2 shows seismic events after removing quarry blasts. Time and location domain discrimination may not be sufficient, hence the vertical component velocity seismogram and spectrum were also examined.

The seismogram and spectrum of the natural and artificial seismic events at ERIK are seen in Figs. 3 and 4, respectively. The P-wave amplitude of artificial seismic events is dominant compared to the amplitude of earthquakes in Fig. 3. In this study, we used some parameters such as the amplitude ratio of the maximum S-wave and maximum P-wave of the vertical component of the velocity seismograms, power ratio (complexity) and total signal duration of the waveform, as described in detail by Horasan et al. 2009. The complexity versus ratio of the maximum P-wave amplitude and maximum S-wave amplitude at the vertical component velocity seismograms of the selected stations

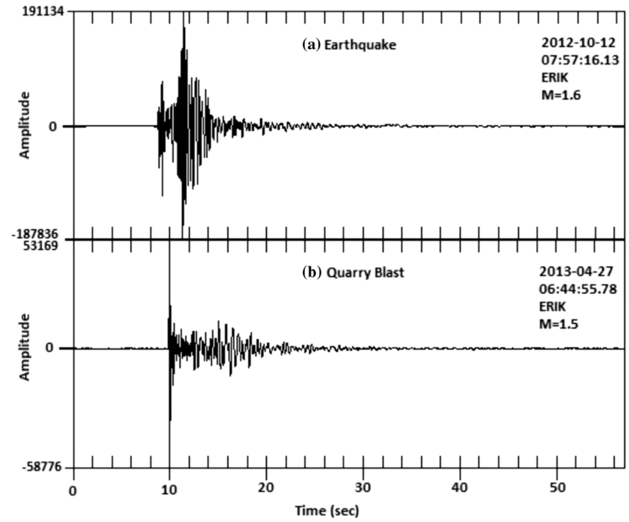

Fig. 3 The vertical component of velocity seismograms recorded at station ERIK. **a** Earthquake, **b** quarry blast

allowed the determination of the linear discriminant function (LDF) using Statistical Package for the Social Sciences (SPSS) Analysis Program (SPSS 2005) to discriminate natural and man-made seismic events.

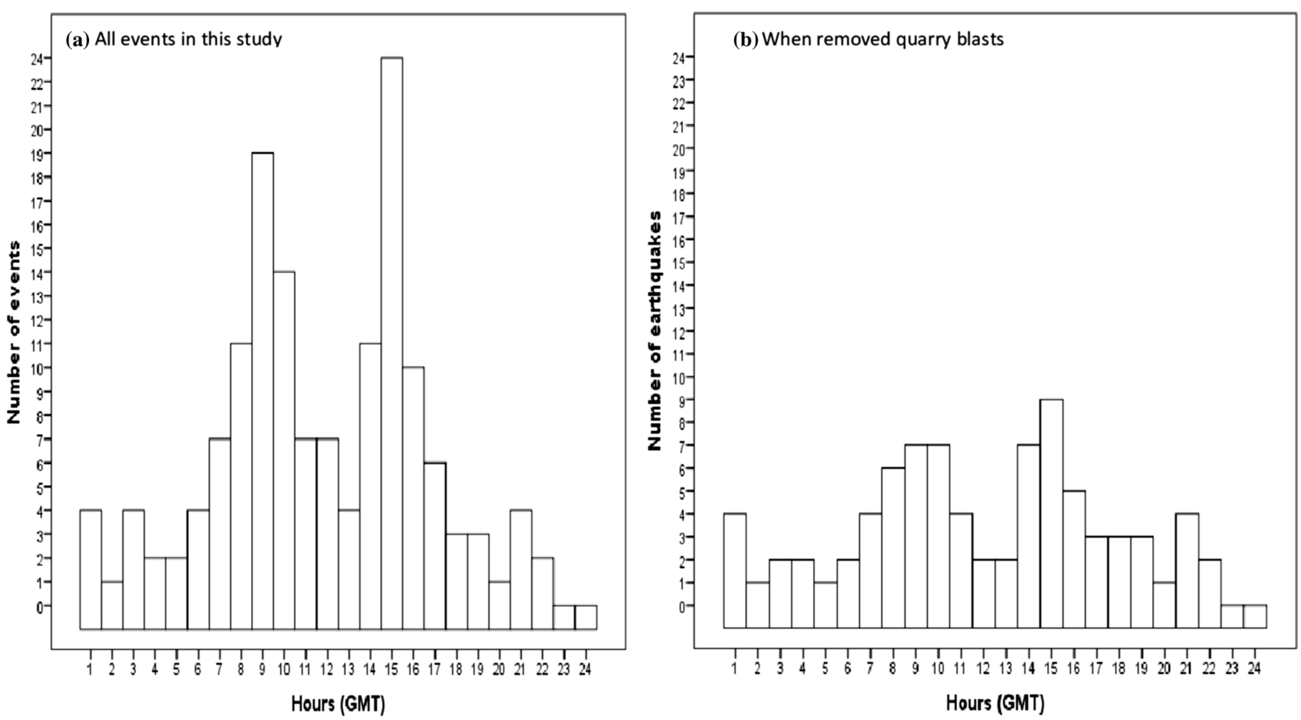

Fig. 2 Distribution of seismic activity (number of events) occurring between May 2009 and March 2104 versus hours (in GMT) in the study area (40–41° N and 25.80–26.70° E). **a** The maximum activity is observed at 09:00 and 15.00 in GMT through the day. **b** Distribution of seismic events after removing quarry blasts

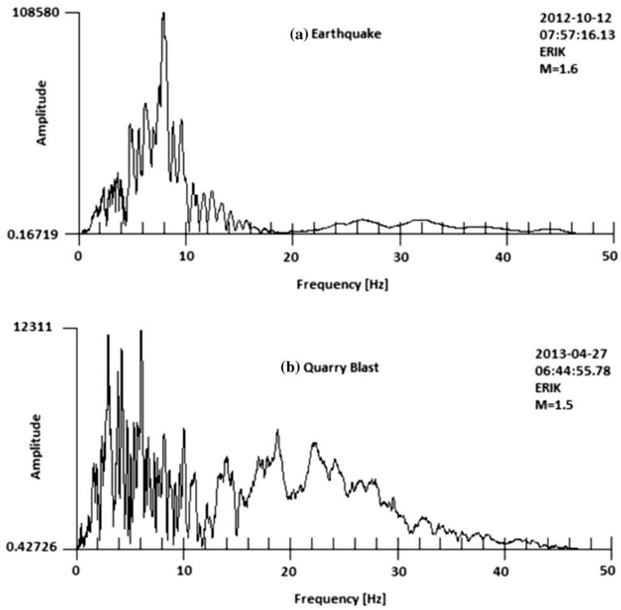

Fig. 4 Normalized amplitude spectrum of signals recorded at station ERIK. **a** Earthquake, **b** quarry blast

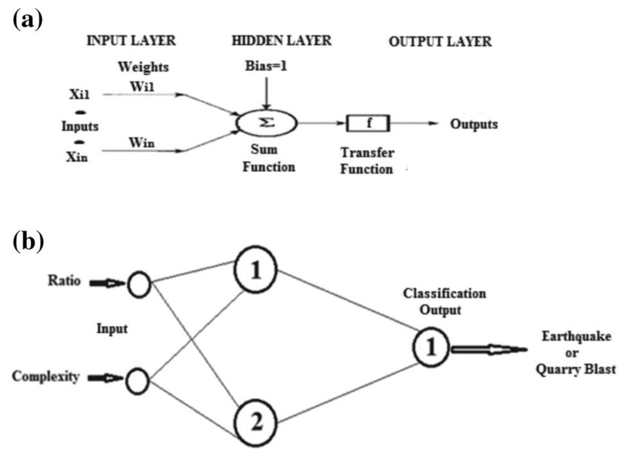

Fig. 5 **a** Members of the network topology, a neural network structure for seismic events. **b** Ratio versus complexity. (Modified from Gülbağ 2006)

Artificial neural networks (ANNs) method

Back propagation feed forward neural networks (BPNNs) learning algorithm

In this study we used the back propagation feed forward neural networks (BPNNs) learning algorithm because of its advantages, such as reducing backward-propagating error, namely from output to input (Çetin et al. 2006) and having an easy neural structure at the expense of slowness in the learning process (Çayakan 2012). According to the size of the errors between the expected output and the real value of the output, weights were organized by using BPNNs learning algorithm in order to obtain the most suitable output values (Yıldırım 2013). Generally, the members of the network topology are shown in Fig. 5 (Gülbağ 2006).

According to the type of the problem, after the learning algorithm was determined, a network structure that included an input layer, a hidden layer and an output layer was obtained. Generally, members of the network architecture were determined as inputs, outputs, weights, the sum function and the activation function (Rumelhart et al. 1986). Inputs were information that entered the cell from other cells or out-medias and entered the cell using connections that were on the weights (w) (Fig. 5).

In this study the topology of the artificial neural network is a feed-forward backpropagation artificial neural network (BPNNs) and its learning algorithm is supervised learning. In the supervised learning algorithm input and output values entered together into the computing system. In this learning algorithm we used the amplitude peak ratio of the S to P-wave and complexity values as input (Fig. 5).

Selection of the number of neurons (Nn)

While deciding the topology of the artificial neural network, the selection of the number of neurons (Nn) is an important criterion in the ANNs method (Gülbağ 2006). Kermani et al. (2005) emphasized that Nn has an important role in neural networks. Nn is one of the significant factors for the discrimination of different data groups. If we used fewer neurons than we needed at the hidden layer, it might cause us to obtain very few sensible results. Often, when the number of neurons is low in hidden layer, it fails to validate the connection of input and output factors. Similarly, when the number of neurons in the hidden layer is high, it causes overfitting (Molga 2003). While the structure of the ANNs was being obtained, Nn was decided by trial and error (Yıldırım 2013; Kaftan et al. 2017).

At the stage of making a decision to determine a suitable model, Nn was tried at an interval and incremented. Then, the artificial neural network model that had the highest accuracy percentage was chosen for the determined ANNs model (Gülbağ 2006). In the literature, researchers used different intervals using different increments. Gülbağ (2006) obtained their ANNs model using increments of 10 neurons between 0 and 100. Küyük et al. (2009) determined their model using increments of 1 neuron between 1 and 20 in the model and selected their number of neurons as 5 because its accuracy percentage was the highest. Yıldırım (2013) obtained their network architecture of ANNs by incrementing the number of neurons by 2 between 0 and 22. Kaftan et al. (2017) determined their model using an increment of 1 between 1 and 6 in their artificial neural network study.

In this study, to define the ANN network we incremented the number of neurons by five between 5 and 25. To determine the best neuron for ANN network we calculated determination coefficient (R^2) values. The highest determination coefficient value is 0.99 for the number of neurons equal to 10 (Table 1). So we selected the best number of neurons as 10 in this data set (Table 1).

An additional training algorithm used was Levenberg–Marquardt, and the activation function used in this study was the Hyperbolic Tangent-Sigmoid activation function. The application of Levenberg–Marquardt to neural network training is described in the literature (Hagan and Menhaj 1994; Kermani et al. 2005). This algorithm has an efficient application in MATLAB software (Charrier et al. 2007; MATLAB 2011). The network trainlm function can train every member of the artificial network (MATLAB 2011). The Levenberg–Marquardt training algorithm has an efficient implementation (Levenberg 1944; Marquardt 1963).

We have to discuss about the training algorithm on a vast scale. Gülbağ and Temurtaş (2007) showed the equations of the standard back propagation and the Levenberg–Marquardt (LM) algorithms. They explained the reasons of using the LM method and the attitudes of that method versus the generalization learning by heart as follows. When the number of the data was inadequate, learning by heart could occure and in that state it might be difficult for the generalization. But according to Gülbağ and Temurtaş (2007) that problem might be solved as: While training with the training set at the same time they were testing it simultaneously by using the test set until an error level determined achieved. When the error of the test set reached to an acceptable level, they recorded the network.

Another activation function selected, denoted by $\varphi(x)$ and defined the output of a neuron in terms of the induced local field v. In this study, we used the hyperbolic tangent sigmoid function in this network architecture. In fact, this activation function assumed a continuous range of values from − 1 to + 1. Therefore, the activation function was an odd function of the induced local field as shown in Eq. (1).

Table 1 The variation of determination coefficient values (R^2) obtained using the ANNs method for the pair of ratio versus complexity parameters that belonged to the Edirne study area versus values of the number of neurons per data set

Data Edrine	Determination coefficient for Nn:5	Determination coefficient for Nn:10	Determination coefficient for Nn:15	Determination coefficient for Nn:20	Determination coefficient for Nn:25
E_ALL	0.97	0.99	0.98	0.97	0.97

$$\varphi(x) = \begin{cases} 1 & \text{if} \quad x > 0 \\ 0 & \text{if} \quad x = 0 \\ -1 & \text{if} \quad x > 0 \end{cases} \tag{1}$$

which is commonly referred to as the signum function. For the corresponding form of a sigmoid function, we may use the hyperbolic tangent sigmoid function, defined by

$$\varphi(x) = \tanh(x) \tag{2}$$

It is a hyperbolic tangent sigmoid activation function to assume positive and negative values as prescribed by Eq. (2) (Haykin 2009).

Based on the initial investigation, the hyperbolic tangent sigmoid was used for all output layers except the first output layer. The hyperbolic tangent sigmoid activation function can be defined using Eq. (3).

$$\varphi(x) = \frac{2}{1 + e^{(-2x)}} - 1 \tag{3}$$

Here: hyperbolic tangent sigmoid activation function

The dynamic variation interval is [− 1 1] and this function shows variations according to the number of neurons and total input (Gradshteyn and Ryzhik 2007).

Preparation of data set

After determining the number of neurons, we started to prepare the data sets that belonged to inputs and outputs. Next, the normalization process was applied. Then, a significant percentage of the data was selected as the training data and the remainder was taken as the testing data. These processes were materialized randomly. Kermani et al. (2005) selected their data randomly in a similar way. We then obtained the new data set. We trained with the training data using the BPNNs learning algorithm. When R^2 was approximately 1, the training was stopped and completed. Next, using the testing process, the ANNs method was applied. This means that "The expected artificial neural network learned the learning algorithm from the training data, so it can test its information using the test data." The data had to provide that rule. The obtained outputs were then compared with the tested outputs. Consequently, the accuracy percentage was calculated.

Different researchers prepared their data using different percentages for training and test data. Ursino et al. (2001) used 50% of their data as training data and 50% of their data as testing data. Gülbağ (2006) used 84% of their data for training and 16% as testing data. Yıldırım et al. (2011) used 25% of their data set as training data and 75% of the data set as testing data for their study. Kundu et al. (2012) used 51% of their data as training data and 49% as testing data in their study. Yıldırım (2013) selected the data randomly and then separated them into two parts. Their training data made up 70% of all data and the remaining part of the data was testing data. Kaftan et al. (2017) selected the data arbitrarily and then separated them into two parts, with 85% of all data used as training data and 15% of the data used as testing data.

In this study the data were randomly selected from all data sets belonging to ERIK, ENEZ and GELI. We arranged a common data set called E_ALL and used 70% of all data as training data and 30% as testing data (Table 2). The all data set consists of 235 seismic events that were recorded in the ERIK, ENEZ and GELI. We then separated the E_ALL data set into two parts. The number of training data points was 165, and the number of test data points was 70 for the E_ALL data set (Table 4).

The ANNs method was applied to a pair of parameters ratio versus C for E_ALL data set and then accuracy percentage was obtained for it (Table 3).

Further, we applied the *k*-fold cross-validation technique to all of the data (James et al. 2017). Suitable results were obtained. All results were obtained using the ANNs method in MATLAB (MATLAB 2011).

Results and discussion

Before we applied the LDF and ANNs methods to the data, we tried to identify earthquake and quarry blasts according to the amplitude of the signal. We observed that the P-wave amplitude of quarry blasts is dominant compared to the amplitude of earthquakes. The frequency content of the events is shown in Fig. 4. We observed the spectral modulation on the quarry blast spectrum. These identification methods were not sufficient for satisfactory discrimination of earthquakes from quarry blasts. For this reason, different pairs of parameters, such as the ratio of the amplitude of the maximum S-wave to the amplitude of the maximum P-wave, the logarithmic value of the amplitude of the maximum S-wave (log *S*), the ratio of power at two time windows of the signal (complexity) and the total duration of the signal were used.

The classification of natural and artificial seismic events was realized using the linear discriminate function (LDF) and the artificial neural networks (ANNs) methods. As a result, 81 (54%) of the total studied 150 seismic events were determined to be earthquakes and 69 (46%) of them were determined to be quarry blasts (Fig. 6).

Ratio versus complexity

The amplitude ratio versus complexity values for the LDF and the ANNs methods are plotted in Figs. 7 and 10 for E_ALL data set. The results of the classification method LDF for pairs of criteria 1 (ratio vs C), 2 (ratio vs log *S*) and 3 (ratio vs duration) are given in Table 5 for the E_ALL data set. In the first criterion in Table 5, 69 earthquakes out of 80 were classified correctly and 11 earthquakes were misclassified as quarry blasts, whereas 155 quarry blasts were classified correctly. Using LDF method we obtained an accuracy percentage of 95% for the E_ALL data set.

After using the LDF method, we discriminated earthquakes and quarry blasts with the ANNs method for the amplitude ratio and complexity parameters. The number of neurons versus the determination coefficient (R^2) for ratio versus Complexity values are given in Table 1. In this table determination coefficient values change between 0.97 and 0.99. The highest value of the determination coefficient (R^2) is a very important criteria for decision of the Nn for the pair of parameters. We selected the best number of neurons as 10 in this data set (Table 1). This situation indicates that the BPNNs learning algorithm is successful for those parameters on that structure of the network architecture. The comparison of determination coefficient (R^2) values that were obtained using the ANNs method for the pair of ratio versus complexity parameters in Edirne and the values of the number of neurons which were increased by 5 between 5 and 25

Table 2 Features of the data set according to the pair of ratio versus complexity parameters using the ANNs method

Data Edrine	Number of all data set	Number of training set	Number of test set	Determination coefficient (R^2)	Number of neurons (Nn)	Accuracy percentage (%) (ANNs)
E_ALL	235	165	70	0.99	10	99

Table 3 Number of events in the training set, test set, misclassified earthquakes and misclassified quarry blasts for the pair of ratio versus complexity parameters according to E_ALL data set using the ANNs method

Criterion	Data Edrine	Number of all data	Number of events in training set	Number of events in test set	Misclassified earthquake (E)	Misclassified quarry blast (QB)	Accuracy percentage (%) (ANNs)
Ratio-C	E_ALL	235	165	70	1	0	99

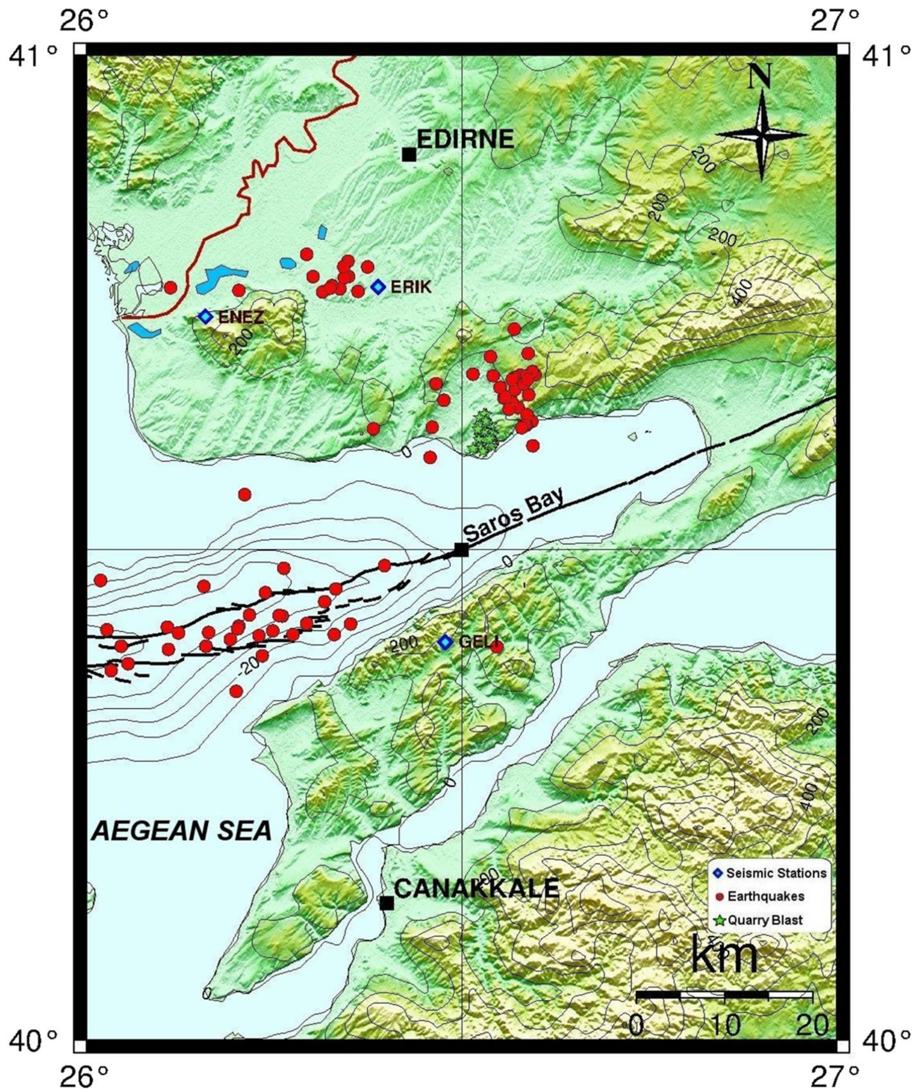

Fig. 6 Distribution of earthquakes (filled red circles) and quarries (filled green stars) in the study area. Faults were taken from Şaroğlu et al. (1992), Emre et al. (2013) and Yaltırak et al. (2012). NAFZ: North Anatolian Fault Zone

is given in Table 1. The comparison of determination coefficient versus Nn is not sufficient for the ANN model performance. In order to evaluate the performance of the model we obtained the variance account value as 99% (Table 2).

We created test and training data set in Table 2. In this study, we used 70% of the total data for training set and 30% for testing (Tables 3, 4). The comparison of the two methods is shown in Table 6.

Ratio versus log *S*

The amplitude ratio versus log *S* values for the LDF method are plotted in Fig. 8 for the E_ALL data set. The results of the classification method between natural and artificial seismic events using the LDF method for criteria pair 2 (ratio vs log *S*) are given in Table 5 for E_ALL data set. In the second criterion in Table 5, 66 earthquakes out of 80 were classified correctly and 14 earthquake were misclassified as a quarry blast, whereas 155 quarry blasts were classified correctly. Using the LDF method we obtained an accuracy percentage of 94% for E_ALL data set.

Ratio versus duration of the signal

The amplitude ratio versus duration of the signal for the LDF method was plotted in Fig. 9 for E_ALL data set. The results of the classification method for natural and artificial seismic events using the LDF method for criteria pair 3 (ratio vs duration) are given in Table 5 for the E_ALL data set. In the third criterion in Table 5, 75 earthquakes out of 80 were classified correctly and 5 earthquakes were misclassified as a quarry blast, whereas 154 quarry blasts were classified

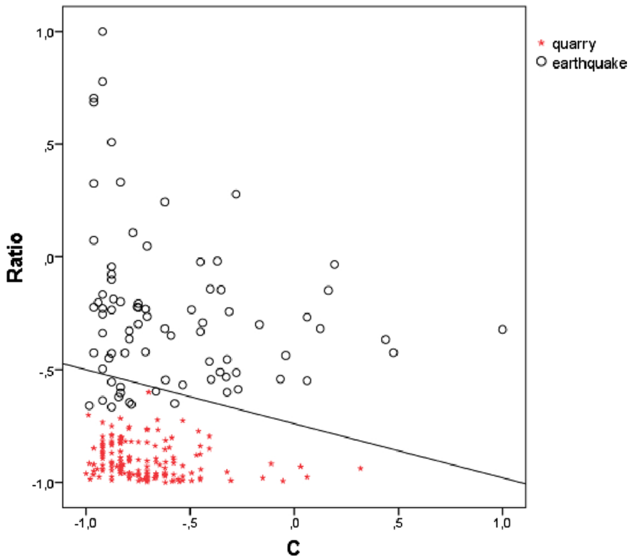

Fig. 7 Plot shows the distribution of ratio versus complexity for the data set including all stations (E_ALL) in the study area. The accuracy percentage obtained is 95% for LDF

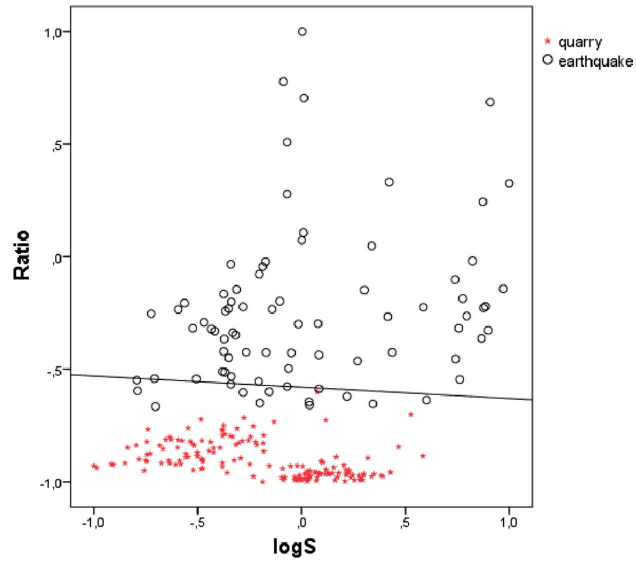

Fig. 8 Plot shows the distribution of ratio versus log S for the data set including all stations (E_ALL) in the study area. The accuracy percentage obtained is 94% for LDF

correctly. Using the LDF method we obtained an accuracy percentage of 97% for the E_ALL data set (Fig. 10).

The LDF method is one of the most popular and successful techniques in earth science worldwide for the classification of natural and artificial seismic events. Horasan et al. (2009) obtained accuracy percentage values for pairs of parameters (Ratio vs log S) of 98.6%, 93.8%, 97.7% and 95.8% for Gaziosmanpaşa, Çatalca, Gebze-Hereke, and Ömerli, respectively. Yılmaz et al. (2013) determined accuracy parameters of 96.3%, 89.3%, 100%, 100%, 96.5%, and 100% for stations KTUT, ESPY, BAYT, PZAR, GUMT, and BCA, respectively, in their study. In their Egypt study, Badawy et al. (2019) obtained lower accuracy percentage values (91.7%, 83.7% and 83.2%) than those seen in other countries using the S-wave/P-wave amplitude peak ratio, complexity and spectral ratio. The accuracy percentage of these parameters depends on the quantity of data, geological features, and local site effects.

Number of neurons versus determination coefficient values for ratio and complexity are given in Table 2. In this table the highest determination coefficient value is 0.99. This situation indicates that the BPNNs learning algorithm was successful for these parameters on that structure of the network architecture in the area considered in this study.

According to the results of this study, the number of seismic events recorded at all three stations by using LDF and ANNs methods will be investigated for whether the accuracy percentage is directly proportional. When we compared the accuracy percentage values for LDF and ANNs methods, both of these methods are successful but the ANNs method is more successful than the LDF method (Table 6). Yıldırım et al. (2011) used three methods to distinguish natural and artificial seismic events in Istanbul and its vicinity. They obtained model success rate of 99% for feed-forward backpropagation neural networks (FFBPNN), 97% for probabilistic neural networks (PNN) and 96% for adaptive neural fuzzy inference systems (ANFIS). These ratios are similar to our E_ALL data set results. Hence, we conclude that the quarry blasts were discriminated very effectively in this study, and this will improve seismic hazard studies of the region. While this is true as a generic principle, the main seismic hazard in the study region is due to the W segment of North Anatolian Fault/NE segment of North Aegean Fault.

Table 4 Number of training and test data sets used for modeling classification status and model accuracy

Criterion	Data Edrine	Number of all data	Training set			Test set		
			Number of events in training set	Earthquake (E)	Quarry blast (QB)	Number of events in test set	Earthquake (E)	Quarry blast (QB)
Ratio-C	E_ALL	235	165	60	105	70	24	46

Table 5 The results of the discriminant analysis using the LDF method for Criterion 1: ratio versus C, Criterion 2: ratio versus log *S* and criterion 3: ratio versus duration parameters for the E_ALL data set

Criterion		Type	Predicted group membership		Total
			Earthquake (E)	Quarry blast (QB)	
1	Original count	E	69	11	80
		QB	0	155	155
	%	E	86.3	13.8	100
		QB	100.0	0.0	100
2	Original count	E	66	14	80
		QB	0	155	155
	%	E	82.5	17.5	100
		QB	0.0	100.0	100
3	Original count	E	75	5	80
		QB	1	154	155
	%	E	93.8	6.3	100
		QB	0.6	99.4	100

The original grouped cases were correctly classified for three criteria at rates of 95%, 94%, and 97% respectively

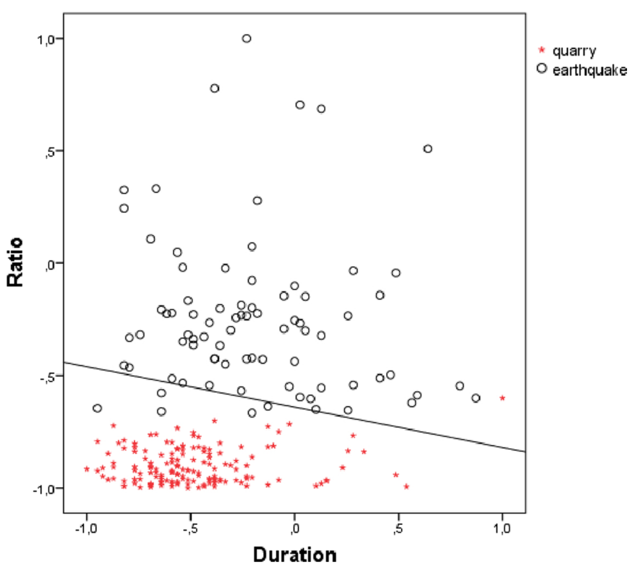

Fig. 9 Plot shows the distribution of ratio versus duration for the data set including all stations (E_ALL) in the study area. The accuracy percentage obtained is 97% for LDF

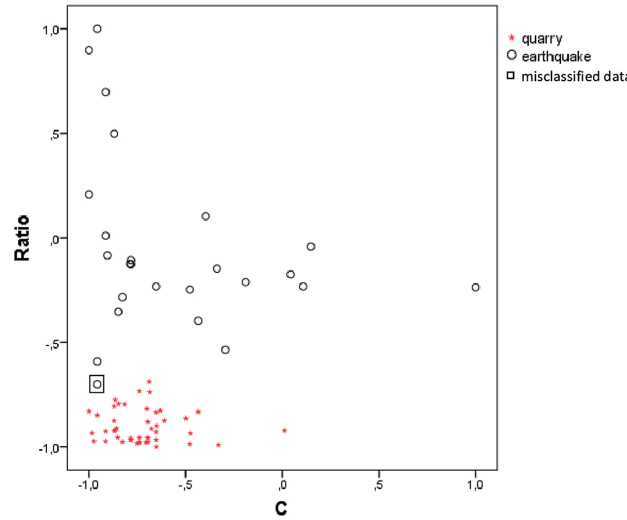

Fig. 10 Plot shows the distribution of ratio versus complexity for the data set including all stations (E_ALL) in the study area. The accuracy percentage obtained is 99% for ANNs

Table 6 Comparison of the accuracy percentage values for the E_ALL data set according to the LDF and ANNs methods

Criteria	Methods	Accuracy (%)
1	LDF	95
	ANNs	99

Acknowledgements We thank the staff of Bogazici University, Kandilli Observatory and the Earthquake Research Institute Regional Earthquake-Tsunami Monitoring Center for sharing the data from the ENEZ, ERIK and GELI stations. We also thank Prof. Dr. Reha Alpar and Res. Assist. Dr. Osman Dağ because of their support on statistical topics and Assistant Prof. Dr. Eray Yıldırım because of his support on the ANNs method. Further, Generic Mapping Tools, GMT, was used to draw the maps (Wessel and Smith 1995).

References

Ataeva G, Gitterman Y, Shapira A (2017) The ratio between corner frequencies of source spectra of P- and S-waves—a new discriminant between earthquakes and quarry blasts. J Seismol 21:209–220

Badawy A, Gamal M, Farid W, Soliman MS (2019) Decontamination of earthquake catalog from quarry blast events in northern Egypt. J Seismol 23:1357–1372

Baumgardt DR, Young GB (1990) Regional seismic waveform discriminants and case-based event identification using regional arrays. Bull Seismol Soc Am 80(Part B):1874–1892

Çayakan Ç (2012) Yapay sinir ağları yöntemiyle sıvılaşma iyileştirmesi için kumlarda uygulanacak kısmi doygunluk tahmini. Yüksek Lisans Tezi, İstanbul Teknik Üniversitesi Fen Bilimleri Enstitüsü İnşaat Mühendisliği EABD Deprem Mühendisliği Bilim Dalı, İstanbul

Çetin M, Uğur A, Bayzan Ş. (2006) İleri beslemeli yapay sinir ağlarında Backpropagation algoritmasının sezgisel yaklaşımı. IV. Bilgelik ve Akademik Bilişim Sempozyumu, 9-11 Şubat 2006, Denizli, Turkey

Ceydilek N, Horasan G (2019) Manisa ve çevresinde deprem ve patlatma verilerinin ayırt edilmesi. Türk Deprem Araştırma Dergisi 1(1):26–47

Charrier C, Lebru G, Lezoray O (2007) Selection of features by a machine learning expert to design a color image quality metrics. In: 3rd international workshop on video processing and quality metrics for consumer electronics (VPQM) 113–119, Scottsdale, Arizona

Deniz P (2010) Deprem ve patlatma verilerinin birbirinden ayırt edilmesi. Yüksek Lisans Tezi, Sakarya Üniversitesi Fen Bilimleri Enstitüsü Jeofizik Mühendisliği EABD, Sakarya

Dowla F, Taylor SR, Anderson RW (1990) Seismic discrimination with artificial neural networks: preliminary results with regional spectral data. Bull Seismol Soc Am 80(5):1346–1373

Emre Ö, Duman, TY, Özalp S, Elmacı H, Olgun S, Şaroğlu S (2013) Active fault map of Turkey with explanatory text. In: General directorate ofmineral research and exploration, Special publication series 30 Ankara, Turkey

Gradshteyn IS, Ryzhik IM (2007) Table of integrals, series, and products, 7th edn. Academic Press, London, pp 28–35

Gülbağ A (2006) Yapay sinir ağı ve bulanık mantık tabanlı algoritmalar ile uçucu organik bileşiklerin miktarsal tayini. Doktora Tezi, Sakarya Üniversitesi Fen Bilimleri Enstitüsü Elektrik-Elektronik Mühendisliği EABD, Sakarya, p 165

Gülbağ A, Temurtaş F (2007) A study on transient and steady state sensor data for identification of individual gas concentrations in their gas mixtures. Sens Actuators B Chem 121(2):590–599

Hagan MT, Menhaj M (1994) Training feed-forward networks with the Marquardt algorithm. IEEE Trans Neural Netw 5(6):989–999

Haykin S (2009) Neural networks and learning machines, 3rd edn. Pearson Prentice Hall Press, p 14. ISBN 9780131471399

Horasan G, Boztepe-Güney A, Küsmezer A, Bekler F, Öğütçü Z (2006) İstanbul ve civarındaki deprem ve patlatma verilerinin birbirinden ayırt edilmesi ve kataloglanması. Proje Sonuç Raporu, Proje No: 05T202, Boğaziçi Üniversitesi Araştırma Fonu

Horasan G, Boztepe-Güney A, Küsmezer A, Bekler F, Öğütçü Z, Musaoğlu N (2009) Contamination of seismicity catalog S by quarry blasts: an example from Istanbul and its vicinity, northwestern Turkey. J Asian Earth Sci 34:90–99

James G, Witten D, Hastie T, Tibshirani R (2017) An introduction to statistical learning with application in R, 7th edn. Springer Publication, Berlin, p 801

Kaftan I, Salk M, Senol Y (2017) Processing of earthquake catalog data of Western Turkey with artificial neural networks and adaptive neuro-fuzzy inference system. Arab Geophys Geosci 10:243

Kalafat D (2010) Türkiye'de Depremlerin Magnitüd-Frekans Uzaysal Dağılımı ve Deprem Kataloğundan Taş Ocağı—Maden Ocağı Patlatmalarının Ayıklanması. Aktif Tektonik Araştırma Grubu 14. Çalıştayı Bildiri Özleri Kitabı, 3-6 Kasım 2010, Adıyaman, p 27

Kartal ÖF (2010) Trabzon and its vicinity deprem ve patlatma verilerinin birbirinden ayırt edilmesi. Yüksek Lisans Tezi, Sakarya Üniversitesi Fen Bilimleri Enstitüsü Jeofizik Mühendisliği EABD, Sakarya, 43s

Kekovalı K, Kalafat D, Deniz P, Kara M, Yılmazer M, Küsmezer A, Altuncu S, Çomoğlu M, Kılıç K (2010) Detection of Potential Mining and Quarry Areas in Turkey Using Seismic Catalog. The 19. Türkiye Uluslararası Jeofizik Kongresi ve Sergisi, 23-26 Kasım 2010, Poster, Ankara

Kekovalı K, Kalafat D, Deniz P (2012) Spectral discrimination between mining blasts and natural earthquakes: application to the vicinity of Tunçbilek mining area, Western Turkey. Int J Phys Sci 7(35):5339–5352

Kermani BG, Schiffman SS, Nagle HG (2005) Performance of the Levenberg–Marquardt neural network training method in electronic nose applications. Sens Actuators B Chem 110(1):13–22

Korrat IM, Gharib AA, Abou Elenean KA, Hussein HM, El Gabry MN (2008) Spectral characteristics of natural and artificial seismic events in the Lop Nor test site, China. Acta Geophys 56(2):344–356

Kundu A, Bhadauria YS, Roy F (2012) Discrimination between earthquakes and chemical explosions using artificial neural networks. Scientific Information Resource Division, BHABHA Atomic Research Centre Technical Report, BARC/2012/E/004, Mumbai, India

Küyük HS, Yıldırım E, Horasan G, Doğan E (2009) Deprem ve taş ocağı patlatma verilerinin tepki yüzeyi, çok değişkenli regresyon ve öğrenmeli vektör nicemleme yöntemleri ile incelenmesi. Uluslararası Sakarya Deprem Sempozyumu, 1-3 Ekim 2009, Kocaeli, 1–10

Küyük HS, Yıldırım E, Doğan E, Horasan G (2011) An unsupervised learning algorithm: application to the discrimination of seismic events and quarry blasts in the vicinity of Istanbul. Nat Hazards Earth Syst Sci 11:93–100

Levenberg K (1944) A method for the solution of certain non-linear problems in least squares. Quart Appl Math 2:164–168

Marquardt DW (1963) An algorithm for least-squares estimation of nonlinear parameters. J Soc Ind Appl Math 11(2):431–441

Molga E (2003) Neural network approach to support modelling of chemical reactors: problems, resolutions, criteria of application. Chem Eng Process Process Intensif 42(8–9):675–695. https://doi.org/10.1016/S0255-2701(02)00205-2

Naserieh S, Karkooti E, Dezvareh M, Rahmati M (2019) Analysis of artifacts and systematic errors of the Iranian Seismological Center's earthquake catalog. J Seismolog 23:665–682

Öğütçü Z, Horasan G, Kalafat D (2010) Investigation of microseismic activity sources in Konya and its vicinity, central Turkey. Nat Hazards 58(1):497–509

Release MATLAB (2011) The neural network toolbox. The MathWorks Inc, Natick

Rumelhart DE, Hinton GE, Williams RJ (1986) Learning internal representations by error propagation. In: Rumelhart D, McClelland JL (eds) vol 1, Chapter 8. MIT Press, Cambridge

Şaroğlu F, Emre O, Kuşçu İ (1992) Active fault map of Turkey. In: Publication of General Directorate of Miner. Res. Explor. Inst. Turkey, Ankara

SPSS V.17.0 (2005) SPSS for Windows. SPSS Inc. (Statistical Package for the Social Sciences)

Telesca L, Lovallo M, Kiszely MM, Toth L (2011) Discriminating quarry blasts from earthquakes in Vértes Hills (Hungary) by using the Fisher–Shannon method. Acta Geophys 59(5):858–871

Ursino A, Langer H, Scarfì L, Grazia GD, Gresta S (2001) Discrimination of quarry blasts from tectonic earthquakes in the Iblean platform (Southeastern Sicily). Ann Geofis 44(4):703–722

Wessel P, Smith WHF (1995) New version of the generic mapping tools (GMT) Version 3.0 released, Transactions. In: American Geophysical Union vol 76. https://doi.org/10.1029/95EO00198

Wüster J (1993) Discrimination of chemical explosions and earthquakes in central Europe-a case study. Bull Seismol Soc Am 83:1184–1212

Yaltırak C, Işler EB, Aksu AE, Hiscott RN (2012) Evolution of the Bababurnu Basin and shelf of the Biga Peninsula: Western extension of the middlestrand of the North Anatolian Fault Zone, Northeast Aegean Sea, Turkey. J Asian Earth Sci 57:103–119

Yavuz E, Sertçelik F, Livaoğlu H, Woith H, Lühr BG (2018) Discrimination of quarry blasts from tectonic events in the Armutlu Peninsula, Turkey. J Seismol 23(1):59–76

Yıldırım E (2013) Sismik dalgaların sönüm karakterinden zemin özelliklerinin belirlenerek sınıflandırılması. Doktora Tezi, Sakarya Üniversitesi Fen Bilimleri Enstitüsü Jeofizik Mühendisliği EABD, Sakarya, p 176

Yıldırım E, Gülbağ A, Horasan G, Doğan E (2011) Discrimination of quarry blasts and earthquakes in the vicinity of Istanbul using soft computing techniques. Comput Geosci 37:1209–1217

Yılmaz Ş, Bayrak Y, Çınar H (2013) Discrimination of earthquakes and quarry blasts in the eastern Black Sea region of Turkey. J Seismol 17(2):721–734